# Dynamics of a microorganism moving by chemotaxis in its own secretion

Ankush Sengupta, Sven van Teeffelen, and Hartmut Löwen

*Institut für Theoretische Physik II: Weiche Materie, Heinrich-Heine-Universität, Universitätsstraße 1, D-40225 Düsseldorf, Germany*
(Received 11 May 2009; revised manuscript received 24 July 2009; published 17 September 2009)

The Brownian dynamics of a single microorganism coupled by chemotaxis to a diffusing concentration field that is secreted by the microorganism itself is studied by computer simulations in spatial dimensions $d = 1, 2, 3$. Both cases of a chemoattractant and a chemorepellent are discussed. For a chemoattractant, we find a transient dynamical arrest until the microorganism diffuses for long times. For a chemorepellent, there is a transient ballistic motion in all dimensions and a long-time diffusion. These results are interpreted with the help of a theoretical analysis.

## I. INTRODUCTION

Chemotaxis [1–3] and Brownian motion [4–6] belong to the key processes that govern the motility of microorganisms (e.g., bacteria, amoeba, and endothelial cells) [7]. In the simplest approach, the microbe "smells" a chemical and moves along the gradient of the concentration field of the chemoattractant in order to reach efficiently the secretion source of the chemical. The opposite case of negative chemotaxis is realized in case the microbe intends to avoid another object that is secreting the chemical [8]. This chemotactic drift is superimposed to stochastic motion due to fluctuations associated with the active process of self-propulsion of the microorganism [9]. Chemotaxis can lead to clusters of aggregated bacteria [10,11] that are still emitting chemoattractant.

Here, we study the self-coupled situation where the microorganism smells itself, i.e., it reacts chemotactically to its own secreted chemical. This "autochemotaxis" is realized in aggregated clusters of different bacteria if the aggregate is considered as a net particle. Another realization is a single bacterium which has both an emitter and a sensor of the same chemical. Tsori and de Gennes [12] have studied a simple model for this situation in different spatial dimensions $d$ and find self-trapping of the bacterium in its own chemoattractant cloud for $d = 1, 2$ but not for $d = 3$. This means that for low dimensionality the bacterium is fooled by its own secretion such that it is getting localized for long times. In a subsequent numerical study of a model microbe coupled to its own chemoattractant secreted at constant rate, Grima [13,14] calculated the long-time dynamics in various dimensions $d$ and found long-time diffusive behavior even for $d = 1, 2$ in contradiction to Ref. [12]. Grima also studied the case of negative chemotaxis and finds in all dimensions long-time diffusion or ballistic motion depending on the strength $\lambda < 0$ which couples the microbe's driving force to the gradient of the chemical concentration field. Grima predicts that if $|\lambda|$ exceeds a critical value $\lambda_c$, then the long-time motion is super-diffusive.

In this paper, we revisit autochemotaxis by studying a model which is similar but not identical to that proposed by Grima [13]. In the model of Grima, a finite global extinction rate ($\Lambda$) of the secreted chemical is present. Here, we focus on the case $\Lambda = 0$, which can be realized in experiments (see, e.g., Ref. [8]). By extensive computer simulations, we study

different spatial dimensions $d = 1, 2, 3$ and both cases of positive and negative chemotaxis. Our results are summarized as follows: consistent with Grima [13], we find for positive chemotaxis (i.e., for a coupling parameter $\lambda > 0$) long-time diffusive motion. In addition we find *dynamical transients* before reaching the long-time diffusive limit. During the transients, the dynamics of the microorganism is strongly reduced resulting in almost dynamical arrest. The crossover time from intermediate arrest to long-time diffusion grows strongly with the coupling $\lambda$. Therefore the idealized analysis of Tsori and de Gennes who predicted self-trapping (i.e., a complete dynamical arrest) is manifested by long transients for very strong couplings [15]. The averaged mean-square displacement as a function of time does not exhibit a universal slope in this transient regime, but the actual mean slope is decreasing with an increase in the coupling $\lambda$. The transient behavior is most pronounced in one dimension but weakened considerably in three dimensions.

For negative chemotaxis (i.e., dynamical self-avoiding of the microbe), on the other hand, we find transient ballistic motion in all dimensions. In $d = 2, 3$ we observe a long-time diffusion for all coupling strength. Such long-time diffusive motion in $d = 1$, though not directly observed in the simulation, is possible by finite probability of changing the direction of motion (left to right) at long-time scales for nonzero temperature. According to Ref. [13], the critical coupling $\lambda_c$ above which ballistic long-time behavior is found depends on the global extinction rate $\Lambda$ but stays finite when $\Lambda \to 0$. One reason for the discrepancy is because noise has not been completely included in the earlier treatments [13], while solving for the integrals concerning the non-Markovian chemotactic force. We take note of the effect of noise on the microbe's trajectory in an appropriate place in this paper (for another example demonstrating the importance of noise, see Ref. [9]). Again we address the transient behavior and find an intermediate time window where the super-diffusive motion is found between a short-time and long-time diffusive behavior. This motion we observe is similar to persistent random walk of a microbe which can be mapped to the wormlike chain model [7,16]. In the particular case we consider, the persistence length is seen to depend on the microbe's coupling with the repellent.

Our predictions can in principle be verified in experiments on aggregates of bacteria. For many bacteria our model reduces to particles interacting via gravitation-kind potentials

for $d=3$. Therefore, our analysis might have applications for Brownian dynamics of gravitational matter [17–19]. Further generalizations of our model are to predator and prey models possibly leading to interesting spatiotemporal delay effects, see, e.g., [20].

Our paper is organized as follows: in Sec. II, we propose the model of a microorganism coupled to its own chemoattractant/chemorepellent, provide the simulation details and point out experimental situations to compare typical estimates of parameters used in the model. In Sec. III we present the results of our investigation. In Sec. IV we explain our findings with simple theoretical analysis. We conclude the paper in Sec. V by discussing the main points of our findings, comparisons of our results with relevant practical cases of self-propulsion, and future directions of our research.

## II. MODEL AND SIMULATION DETAILS

*Model:* The microorganism is modeled as a point particle which undergoes completely overdamped Brownian motion with an effective temperature $\beta^{-1}$ in a medium with viscosity coefficient $\gamma$. This "particle" is assumed to emit a chemical, with which it is self-coupled, continuously in time. In this context, the word "particle" is thereby taken to represent the chemotactic agent of interest–an idealized microorganism coupled with a self-emitted chemical field. Fluctuations associated with the active process of self-propulsion of the microbe is modeled by the effective temperature parameter $\beta^{-1}$ in our system. The time evolution of the density field $\rho(\mathbf{r},t)$ of the continuously emitted chemical is thus governed by a diffusion equation with a source term that depends upon the instantaneous position $\mathbf{r}_b(t)$ of the moving microbe

$$\frac{\partial \rho(\mathbf{r},t)}{\partial t} = D_c \nabla^2 \rho(\mathbf{r},t) + \lambda_e \delta[\mathbf{r} - \mathbf{r}_b(t)]. \quad (1)$$

Here, the constants $\lambda_e$ and $D_c$ are the rate of emission of the chemical and the diffusion constant of the chemical in the medium, respectively.

In the absence of chemical, the microbe diffuses nonchemotactically in the medium with an effective free diffusion constant $D=1/(\gamma\beta)$. However, with the presence of the emitted chemical, the resulting "chemotactic" behavior depends on the nature of the self-coupling of the microorganism to its chemical field, i.e., whether it moves "up" or "down" the chemical density gradient. We study both cases by simply modeling the self-coupling "force" to be proportional to the gradient of the chemical density field $\nabla\rho(\mathbf{r},t)$, and the proportionality constant $\lambda$ determines the strength as well as the nature of the coupling. In reality, of course, chemotaxis can be more complex involving temporally sampling of the concentration field and a biased random walk [7,21,22]. In this context, we note that the "chemotactic force" imitates the net effect of chemotactic movements on a phenomenological level. The details of the actual propulsion mechanism [23] of the chemotactic agent and the effect of the solvent flow field on the diffusing chemical are not taken into account. Within our simple model, positive and negative $\lambda$ naturally generate the cases of positive and negative

chemotaxes, respectively. We are thus led to the following idealized model of a chemotactic agent:

$$\gamma \dot{\mathbf{r}}_b(t) = \mathbf{F}(\mathbf{r}_b,t) + \boldsymbol{\eta}(t). \quad (2)$$

Here, $\boldsymbol{\eta}(t)$ is an effective noise specified by $\langle \boldsymbol{\eta}(t) \rangle = 0$ and $\langle \eta_i(t) \eta_j(t') \rangle = 2\gamma\beta^{-1}\delta_{ij}\delta(t-t')$, with $i$ and $j$ referring to the spatial components of the noise vector. This noise term is assumed to effectively take care of all nonequilibrium fluctuations that may be associated with the *active* process [24,25] of self-propulsion, in absence of the chemical. $\mathbf{F}(\mathbf{r}_b,t)$ denotes the model chemotactic force taken to imitate the systematics of the effective chemotactic movement of the microbe at the position $\mathbf{r}_b$ at time $t$ due to the chemical secreted all along the trajectory traversed in the past. It is obtained by analytically solving Eq. (1) for the density field $\rho(\mathbf{r},t)$ by the method of Green's function, and subsequently calculating the gradient $\nabla\rho(\mathbf{r},t)$. The "force" at a time instant is dependent on the entire previous path history of the microorganism, thereby generating a strongly non-Markovian dynamics. However, owing to a physical *memory time* ($t_0$) associated with the microbe to sense its chemical, the part of the trajectory in this most recent time $t_0$, i.e., for all $\mathbf{r}_b(t')$ with $t-t_0 < t' \leq t$, does not contribute. The physical import of this is that there is a finite time delay $t_0$, however small, between the act of secreting chemical by the microorganism and the act of responding to it, during which the sensor gets to activate. With the introduction of the memory time, $t_0$, the chemotactic force at time $t$ and at position $\mathbf{r}$ becomes

$$\mathbf{F}(\mathbf{r},t) = -2\lambda\lambda_e \int_0^{t-t_0} dt' \frac{(\mathbf{r} - \mathbf{r}_b(t'))}{4D_c|t-t'|} \frac{\exp\left[\frac{-(\mathbf{r} - \mathbf{r}_b(t'))^2}{(4D_c|t-t'|)}\right]}{(4\pi D_c|t-t'|)^{d/2}}, \quad (3)$$

where $d$ is the dimensionality of the embedding space. Evidently form Eq. (3), for the mathematical case of $t_0=0$, the "force" becomes divergent.

*Simulation details:* We performed extensive Brownian dynamics simulation [26] for this non-Markovian process of a microorganism moving by autochemotaxis. We measured time in units of $\tau_0 = \lambda_e^{-1}$, all lengths in units of $l_0 = (\sqrt{DD_c}/\lambda_e)^{1/2}$ and energies in units of $\beta^{-1}$. The coupling strength $\lambda$ is measured in units of $\beta^{-1}l_0^d$. Thus, we set $\lambda_e=1$, $l_0=1$ and $\beta=1$ for convenience. Further we considered the physical situation when the microorganism diffuses at a much slower rate compared to the emitted chemical in the medium [27,28], taking $D=0.1\ l_0^2/\tau_0$ and fixing the ratio $D/D_c=0.01$. In our Brownian dynamics simulations we used $t_0=0.001\tau_0$. The Langevin equation [Eq. (2)] is solved with a discrete time step $\Delta t=0.0001\tau_0$. Space is, however, continuous.

*Connection to experiments:* In order to get an estimate for the coupling strength $\lambda$ in our units, we note that the typical value of the ejection rate of chemical from a microorganism is $\lambda_e \sim 10^3$ molecules/s [12,29], and usually $D/D_c \sim 10^{-1}-10^{-2}$ [27,28]. In three spatial dimensions, for example, the chemotaxis of *Dictyostelium* to shallow cAMP gradients [30,31] with typical values of $\nabla\rho \sim 0.01$ nM/$\mu$m, $D_c \sim 300\ \mu$m$^2$/s, $D/D_c \sim 10^{-2}$, and moving with steady-

state velocity $v \sim 0.2$ $\mu$m/s, yields $\lambda \sim 10^4 \beta^{-1} l_0^3$.

Chemotactic *Microglia* cells [28] move at a speed of $v \sim 2$ $\mu$m/min in a spatial gradient $\nabla \rho \sim 0.003$ nM/$\mu$m of a chemoattractant (IL$-1\beta$), which is secreted at a rate of $\lambda_e \sim 200$ molecules/min and diffuses with $D_c = 900$ $\mu$m$^2$/min. The coupling strength in this case is $\lambda \sim 10\beta^{-1} l_0^3$ for an effective nonchemotactic diffusion constant $D \sim 33$ $\mu$m$^2$/min of microglial cells, due to random motility in the tissue. The chemoattractant has a low decay rate of $\Lambda \sim 0.003 - 0.03$ min$^{-1}$. Microglial cells are also known to respond to a chemorepellent (TNF$-\alpha$) they produce, with similar production, diffusion and decay rates as the chemoattractant. Our estimate of the chemoattractant gradient was based on the value of the chemotactic coefficient $\sim 780$ $\mu$m$^2$ nM$^{-1}$ min$^{-1}$, a ratio between cell velocity and chemical gradient, used in Ref. [28]. The corresponding value for the repellent is not known.

Again, for *E. coli* of size $\sim 1$ $\mu$m, swimming at $v \sim 20$ $\mu$m/s in the spatial gradient $\nabla \rho \sim 0.1$ $\mu$M/$\mu$m of a chemoattractant diffusing with $D_c = 10^{-5}$ cm$^2$/s, in a medium of viscosity $10^{-3}$ Pa.s [32,33]; the coupling strength is $\lambda \sim 10^{-1}$ $\beta^{-1} l_0^3$. The nonchemotactic diffusion coefficient of the bacterium is $D = 6.6 \times 10^{-6}$ cm$^2$/s. The time required by the chemical in this case, to diffuse a length equal to the size of the bacterium, is on the order of $0.1$ $\tau_0$. The memory time $t_0$, needed by the bacterium to respond to the chemical stimulus, can be much smaller than this time.

In all the above calculations, the effective nonchemotactic diffusivity $D$ was used to express the energy unit $\beta^{-1} = \gamma D$.

## III. RESULTS

We now investigate the nature of the dynamics in all the dimensions and for both cases of positive and negative $\lambda$, examining the model microorganism from some initial reference point taken as the origin, i.e., $\mathbf{r}_b(t=0) = 0$. For this purpose, we computed the mean-square displacement of the microbe as a function of time and averaged over $10^3$ realizations for each case. We checked that the system is in a steady state, and have also performed a steady state averaging of the mean-square displacement. We illustrate our findings below.

### A. Positive autochemotaxis

Upon examining the motion of the microbe in a chemoattractant ($\lambda > 0$) in one dimension ($d=1$), we found signatures of long-time diffusion $\{\langle [\mathbf{r}_b(t) - \mathbf{r}_b(0)]^2 \rangle \sim t\}$ with a modified diffusion constant $D_l$. The value of $D_l$ depends on the strength of the coupling $\lambda$, and decreases with increasing $\lambda$. For very high $\lambda$ values, it is computationally difficult to obtain the long-time diffusive behavior; but we obtained an upper estimate of the diffusivity for lower $\lambda$ values from a fit to the obtained data. In the opposite limit, i.e., at very short times, the microbe's dynamics is also diffusive with the nonchemotactic diffusion constant $D$. The departure from this behavior occurs at times dependent on the coupling strength: the stronger the coupling, the dynamics becomes markedly history dependent and the microorganism deviates

from the nonchemotactic diffusion faster. At intermediate times, we find long period of subdiffusive crossover regime, showing signatures of a transient dynamical arrest at high $\lambda$ values. The crossover time also increases with the coupling strength. Figure 1(a) shows the mean-square displacement as a function of time in $d=1$, for three values of $\lambda$ and compared with the nonchemotactic diffusion.

In $d=2$, we find similar long-time diffusive behavior. The crossover times from early-time nonchemotactic diffusion to the long-time modified diffusion is greatly reduced for a given $\lambda$ value as compared to the one-dimensional case. This feature is attributed to the effect of fluctuations. The crossover time to the final long-time diffusion, however, increases with coupling strength. The intermediate subdiffusive regime is also diminished in time. The mean-square displacement as a function of time, in this case, is shown in Fig. 1(b).

In Fig. 1(c), we show the case for $d=3$, and in consistence with our expectation, we find similar long-time diffusion with a further reduced crossover time as compared to the low-dimensional cases. Thus, the transient dynamical arrest becomes more prominent at lower dimensions and at stronger couplings. The $\lambda$ dependence of the modified diffusion constant $D_l$, is shown in Fig. 1(d), for all dimensions, relative to the corresponding nonchemotactic diffusion constant $D$.

### B. Negative autochemotaxis

For the repulsive case, when the model microorganism gets repelled by its ejected chemical ($\lambda < 0$), we found a short-time nonchemotactic diffusive motion with a crossover to a ballistic behavior $\{\langle [\mathbf{r}_b(t) - \mathbf{r}_b(0)]^2 \rangle \sim t^2\}$ in one dimension, for all values of the coupling strength [Fig. 2(a)]. The time of commencement of the ballistic behavior, however, depends on $\lambda$. For weak coupling (i.e., low $|\lambda|$), the dynamics resembles the nonchemotactic diffusion for longer times before finally going over to the ballistic dynamics. The velocity of this ballistic motion is given by the time derivative of the root mean-square displacement, $\frac{\partial}{\partial t}\sqrt{\langle [\mathbf{r}_b(t) - \mathbf{r}_b(0)]^2 \rangle}$, and this velocity is seen to increase with increase in the coupling strength $|\lambda|$. We argue that the microorganism can change the direction of its motion in one dimension due to a nonvanishing finite barrier crossing probability. Under such circumstance, the motion will be diffusive at very long times (not seen in the simulation), with higher diffusion constant.

In higher dimensions $d=2$ [Fig. 2(b)] and $d=3$ [Fig. 2(c)], we observed a crossover from the nonchemotactic diffusion to a long-time diffusion for all coupling strengths, with a ballistic transient dynamics at intermediate times for high $|\lambda|$. The velocity of the transient ballistic motion increase with increasing coupling strength. The time duration of this ballistic transient as well as the modified long-time diffusion constant are also $\lambda$-dependent, both increase with increase in $|\lambda|$. In Fig. 2(d) we show this modified diffusion constant for the repulsive case relative to the nonchemotactic diffusion constant as a function of $|\lambda|$, in $d=2,3$.

## IV. THEORY

Our findings can be understood qualitatively and partly quantitatively by relatively simple theoretical considerations,
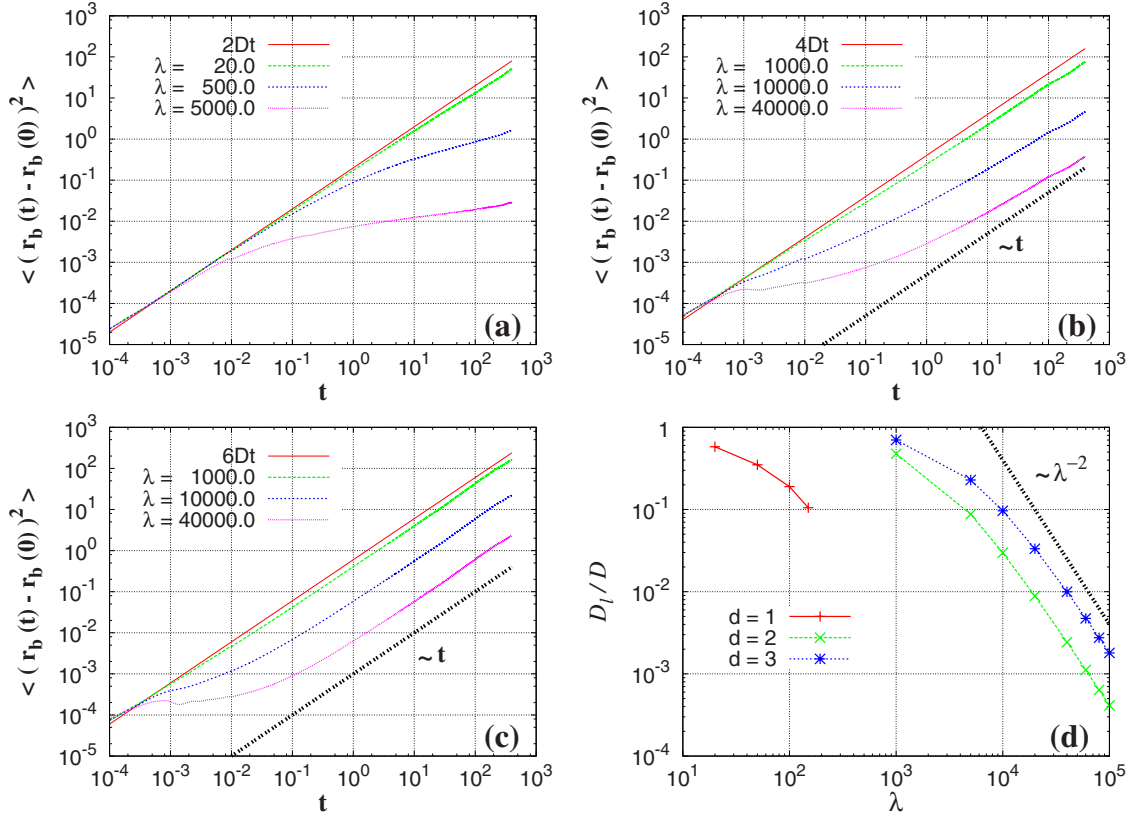
FIG. 1. (Color online) Mean-square displacement $\langle[\mathbf{r}_b(t) - \mathbf{r}_b(0)]^2\rangle$ of the microorganism as a function of time $t$ with chemoattractant in (a) $d=1$ with $\lambda=20, 500, 5000$; (b) $d=2$ with $\lambda=1000, 10000, 40000$; (c) $d=3$ with $\lambda=1000, 10000, 40000$. The nonchemotactic diffusion reference lines are also indicated as $2Dt$, $4Dt$, and $6Dt$ correspondingly for $d=1,2,3$. Reference lines (thick dotted) are used to indicate the long-time diffusive behavior ($\sim t$) wherever possible. The relative long-time diffusivity $D_l/D$ is shown as a function of $\lambda$ in (d) for $d=1,2,3$. The reference line (thick dotted) shows a power-law scaling behavior $\sim 1/\lambda^2$ (see text).

which are presented in the current section. In Sec. IV A, a scaling law for the diffusion constant for the case of positive chemotaxis $D_l \propto D_c^{d+2} t_0^{d-2}/\lambda^2$, is derived based on a simple rate theory. The same scaling $D_l \propto \lambda^{-2}$ had been predicted for the slightly different model, which includes evaporation, by Newman and Grima [34] and Grima [13]. In Sec. IV B, we present a theory, which quantitatively predicts the long-time diffusion constant in the case of negative chemotaxis for all coupling strengths.

Both approaches, for negative and positive chemotaxis, attribute the long-time diffusion to small fluctuations about the respective steady states in the case of zero noise. In each subsection, we therefore first present the solutions to the equation of motion (2) without fluctuations (i.e., at zero temperature or infinite coupling strength $\lambda$), before discussing the influence of small fluctuations on the long-time dynamics.

### A. Positive autochemotaxis

In the case of strong positive autochemotaxis, the model microorganism is trapped within its own secretion, which effectively provides an attractive external potential at the microbe's location $\mathbf{r}_b(t)$. For zero noise, the microbe is at rest, i.e., $\mathbf{r}_b(t)=\mathbf{r}_b$, and does not experience any force. If, on the contrary, the microbe was at time $t$ instantaneously placed a

distance $\mathbf{r}-\mathbf{r}_b$ away from the location, which it occupied at all earlier times $t'<t$, it would feel a force $\mathbf{F}_s(\mathbf{r})$, which is obtained analytically by evaluating Eq. (3) (see also Fig. 3)

$$\mathbf{F}_s(\mathbf{x}) = \begin{cases} -\dfrac{\lambda}{2D_c}\mathrm{erf}(x)\dfrac{\mathbf{x}}{x}, & d=1 \\[2ex] -\dfrac{\lambda}{4\pi D_c^2 t_0}(1 - e^{-x^2})\dfrac{\mathbf{x}}{x^2}, & d=2 \\[2ex] -\dfrac{\lambda}{4\pi^{3/2} D_c^2 t_0}\left[\dfrac{\sqrt{\pi}}{2x}\mathrm{erf}(x) - e^{-x^2}\right]\dfrac{\mathbf{x}}{x^2}, & d=3. \end{cases}$$
(4)

Here, $\mathbf{x}=(\mathbf{r}-\mathbf{r}_b)/(2\sqrt{D_c t_0})$ is the dimensionless distance from the former position $\mathbf{r}_b$ of the microbe and $x=|\mathbf{x}|$ is its absolute value. Locally, i.e., for distances $|\mathbf{r}-\mathbf{r}_b| \ll 2\sqrt{D_c t_0}$, the force is linear in the distance and given by

$$|\mathbf{F}_s(\mathbf{r})| \simeq \begin{cases} (2\sqrt{\pi D_c^3 t_0})^{-1}\lambda|(\mathbf{r}-\mathbf{r}_b)|, & d=1 \\[1.5ex] (8\pi D_c^2 t_0)^{-1}\lambda|(\mathbf{r}-\mathbf{r}_b)|, & d=2 \\[1.5ex] (24\sqrt{\pi^3 D_c^5 t_0^3})^{-1}\lambda|(\mathbf{r}-\mathbf{r}_b)|, & d=3. \end{cases}$$
(5)

Without fluctuations, the microbe never experiences the described force field. However, if the noise is nonzero but small, the microbe eventually walks up the locally parabolic
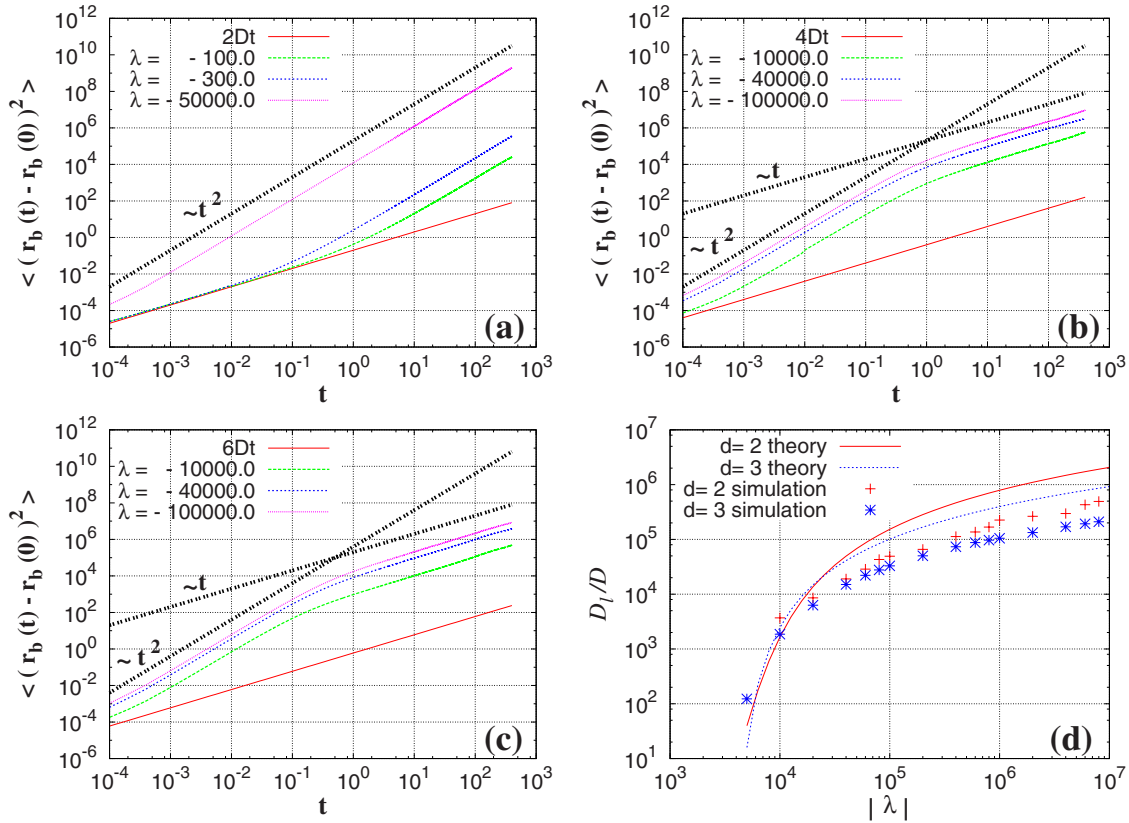
FIG. 2. (Color online) Mean-square displacement $\langle[\mathbf{r}_b(t)-\mathbf{r}_b(0)]^2\rangle$ of the microorganism as a function of time $t$ with chemorepellent in (a) $d=1$ with $\lambda=-100,-300,-50000$; (b) $d=2$ with $\lambda=-1000,-40000,-100000$; (c) $d=3$ with $\lambda=-1000,-40000,-100000$. The nonchemotactic diffusion reference lines are also indicated as $2Dt$, $4Dt$, and $6Dt$ correspondingly for $d=1,2,3$. Reference lines (thick dotted) indicating the ballistic ($\sim t^2$) and the long-time diffusive ($\sim t$) dynamics is shown as guide to the eye. The relative long-time diffusivity $D_l/D$ is shown as a function of $|\lambda|$ in (d) for $d=2,3$. The points represent the actual data obtained from simulations, the lines correspond to a semiquantitative theory (see text).

walls of its self-generated potential for a short time $\tau$, which, in turn, might lead to a shift in the position of the minimum $\mathbf{r}_0$ of the self-generated attractive potential by a distance $\Delta\mathbf{r}_0=\mathbf{r}_0(t+\tau)-\mathbf{r}_0(t)$. Clearly, the minimum is only displaced, if the duration of the excursion $\tau$ is larger than the memory time $t_0$ and if the microbe excurses predominantly in one direction. After time $t+\tau$ the microbe position might relax to the new minimum, $\mathbf{r}_b(t'>t+\tau)\rightarrow\mathbf{r}_0(t+\tau)$. By such a fluctuation, the microorganism effectively manages to move a distance $\Delta\mathbf{r}_0$ within the time $\tau$.

Most relevant for the long-time diffusion are those fluctuations, which yield a large displacement $\Delta\mathbf{r}_0$ and still occur at a high-rate $\gamma_R\lesssim 1/\tau$. These fluctuations are regarded to constitute the relevant mean steps in an effective continuous time random walk with the desired diffusion constant $D_l\sim\Delta\mathbf{r}_0^2/\tau$.

In this subsection, we only attempt to obtain a scaling law for the long-time diffusivity. We therefore restrict our consideration to a subset of very simple fluctuations, which are believed to be representative for all fluctuations relevant for diffusion. In particular, we consider a "jump" process at time $t=0$: at all earlier times, $t<0$, the microbe is resting at the location of the self-generated potential's minimum at the origin, i.e., $\mathbf{r}_b(t<0)=\mathbf{r}_0(0)=\mathbf{0}$, before it undergoes an excursion to a new location $\mathbf{r}_b(\epsilon<t<\tau)=\Delta\mathbf{r}_b$ within a time $\epsilon$; the latter

time scale is assumed to be small with respect to the residence time $\tau$. During the latter time span $\tau$, the microbe stays at the new position, where it resists the force due to the secretion from earlier times. In the case of a large coupling strength $\lambda$, the process of getting to the new location during the time span of duration $\epsilon$ is irrelevant. After time $\tau$, the position of the model microbe is deterministically relaxing
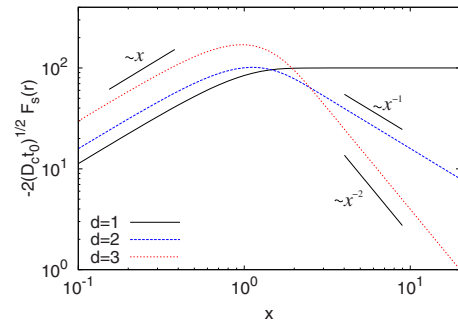


FIG. 3. (Color online) The force $|\mathbf{F}_s(\mathbf{r})|$, which a microorganism would experience if it was at time $t$ instantaneously placed a distance $\mathbf{r}-\mathbf{r}_b$ away from the location, which it occupied at all earlier times $t'<t$, plotted as a function of $x=|\mathbf{r}-\mathbf{r}_b|/(2\sqrt{D_ct_0})$ for all dimensions $d=1,2,3$. Representative parameters chosen are $D_c=0.1$, $t_0=0.01$, and $\lambda=10^4$.

toward the new minimum of the chemoattractant at $\Delta \mathbf{r}_0(\tau, \Delta \mathbf{r}_b) < \Delta \mathbf{r}_b$, which is a function of the parameters $\tau$ and $\Delta \mathbf{r}_b$, only. Summarizing, the simple pathway is described by

$$\mathbf{r}_b(t) = \begin{cases} \mathbf{r}_b(0) = \mathbf{0}, & t < 0 \\ \Delta \mathbf{r}_b, & \epsilon < t < \tau \\ \Delta \mathbf{r}_0(\tau), & t > \tau. \end{cases} \quad (6)$$

The probability of the described fluctuation is proportional to the Arrhenius factor [35]

$$p[\tau, \Delta r_b] \propto \exp[-S(\tau, \Delta r_b)/4], \quad (7)$$

with $\Delta r_b = |\Delta \mathbf{r}_b|$ and $S(\tau, \Delta r_b)$ the Onsager-Machlup action

$$S(\tau, \Delta r_b) = \gamma \int_0^\tau dt |\dot{\mathbf{r}}_b(t) - \gamma^{-1} \mathbf{F}(t)|^2. \quad (8)$$

Neglecting the initial process of moving the distance $\Delta r_b$ and also ignoring the relaxation of the chemoattractant during the time $\tau$ the action is approximately given by

$$S(\tau, \Delta r_b) \approx \gamma^{-1} \tau [\mathbf{F}_s(\Delta r_b)]^2, \quad (9)$$

which, together with Eqs. (4) and (5), yields

$$S(\tau, \Delta r_b) \propto \begin{cases} \dfrac{\lambda^2 \Delta r_b^2 \tau}{\gamma D_c^2 (D_c t_0)^d}, & \Delta r_b \ll 2\sqrt{D_c t_0} \\ \dfrac{\lambda^2 \tau}{\gamma D_c^2 \Delta r_b^{2(d-1)}}, & \Delta r_b \gg 2\sqrt{D_c t_0}. \end{cases} \quad (10)$$

According to Eq. (7), a minimum requirement for the described fluctuation to occur frequently is that $S(\tau, \Delta r_b)$ does not exceed a value on the order of 1, i.e., $S(\tau, \Delta r_b) \lesssim 1$. As Eq. (10) is a strictly monotonically increasing function of $\tau$ and $\Delta r_b$, this constraint is equivalent to the equality

$$S(\tau, \Delta r_b) = 1. \quad (11)$$

Diffusion is believed to be governed by those random displacements of the microorganism, which maximize the shift in the potential's minimum $\Delta r_0(\tau, \Delta r_b) = |\Delta \mathbf{r}_0(\tau, \Delta \mathbf{r}_b)|$ subject to this constraint.

We will shortly see that for large coupling constants $\lambda^2 \gg D_c^{d+1} t_0^{d-2} \gamma$, small excursions $\Delta r_b \leq 2\sqrt{D_c t_0}$ are most relevant. In this latter limit, $\Delta r_0$ is obtained analytically as

$$\Delta r_0(\tau, \Delta r_b) \simeq [1 - (t_0/\tau)^{d/2}] \Delta r_b. \quad (12)$$

The maximum of $\Delta r_0$ subject to the constraint of Eq. (11) is given by

$$\Delta r_0^* \simeq \frac{d}{d+1} \Delta r_b^*, \quad (13)$$

at an optimum displacement of the microbe and an optimum residence time

$$\Delta r_b^* \simeq a \sqrt{\gamma D_c^{d+2} t_0^{d-1}} / \lambda,$$

$$\tau^* \simeq b t_0, \quad (14)$$

with prefactors $a = 2^{-1}, 3^{-1/2}, 2^{-2/3}$ and $b = 4, 3, 2^{4/3}$ in one, two, and three dimensions, respectively. Clearly, Eq. (14)

fulfills the before-mentioned assumption of small excursions in the limit of large $\lambda^2 \gg D_c^{d+1} t_0^{d-2} \gamma$. Equation (14) yields the desired scaling behavior for the long-time diffusivity $D_l \propto \Delta r_0^2 / \tau$,

$$D_l \propto \frac{\gamma D_c^{d+2} t_0^{d-2}}{\lambda^2}. \quad (15)$$

In conclusion, the simple theory predicts an inverse quadratic dependence of $D_l$ on $\lambda$ in the strong-coupling limit, which has also been observed in the computer simulations [see Fig. 1(d)]. The same scaling had already been predicted for the slightly different model, which includes evaporation, by Newman and Grima [34] and Grima [13].

### B. Negative autochemotaxis

First, we consider the microorganism's motion with no fluctuations present. In this case, the swimmer reaches a steady state at infinite time, which is determined by a constant swimming speed $\dot{\mathbf{r}}_s(t \to \infty) = \mathbf{v}_s$, where the index $s$ denotes the steady-state configuration. Under this condition, the drag force induced by the solvent, $\gamma \mathbf{v}_s$, equals the driving force due to the chemical, $-\lambda \nabla \rho$. Figuratively, the microorganism surfs down its own chemorepellent, which it excreted at times $t' < t - t_0$. Using Eq. (3), the steady-state velocity $v_s$ is determined by the self-consistent equation

$$\gamma v_s = -\frac{\lambda v_s}{2 D_c} \int_{t_0}^\infty dt' \frac{\exp[-v_s^2 t'/(4 D_c)]}{(4\pi D_c t')^{d/2}}$$
$$= \left(\frac{v_s}{4\pi^{1/2} D_c}\right)^d \frac{2\lambda}{v_s} \Gamma\left(1 - \frac{d}{2}, \frac{v_s^2 t_0}{4 D_c}\right), \quad (16)$$

where $\Gamma(a, z)$ denotes the incomplete gamma function. Equation (16) has nonzero solutions $v_s > 0$ for any value of $\lambda$ in one and two spatial dimensions, whereas there is a dynamical phase transition at a lower critical value of $\lambda^* = -8\pi^{3/2} D_c^{5/2} t_0^{1/2} \gamma$ in three dimensions, below which the microbe comes to a rest. The latter is obtained analytically by expanding Eq. (16) up to second order in $v_s$. For the parameters used in the simulations reported above, $D_c = 10$, $\gamma = 10$, and $t_0 = 0.001$, the transition occurs at $\lambda^* \approx -4450$. The asymptotic solutions for small $|\lambda|$ in one and two dimensions or for small $|\lambda - \lambda^*|$ in three dimensions, respectively, are given by

$$v_s(\lambda) \simeq \begin{cases} (2 D_c \gamma)^{-1} |\lambda|, & d = 1 \\ 2(D_c/t_0)^{1/2} \exp\left[-\dfrac{\gamma_E}{2} - \dfrac{4\pi D_c^2 \gamma}{|\lambda|}\right], & d = 2 \\ (4\pi^2 D_c^2 \gamma t_0)^{-1} (|\lambda - \lambda^*|), & d = 3, \end{cases} \quad (17)$$

where $\gamma_E \approx 2.7183$ is Euler's constant. The steady-state velocity as a function of $|\lambda|$ is shown in Fig. 4 for all three spatial dimensions. For high coupling constants, $\lambda \gtrsim 10^4$, the steady-state velocities $v_s$ agree well with the square root of the slope of the mean-square displacements $v_s \approx \partial \sqrt{\langle [\mathbf{r}_b(t) - \mathbf{r}_b(0)]^2 \rangle} / \partial t$, as obtained from the simulations with noise in two and three dimensions (see also Fig. 4).
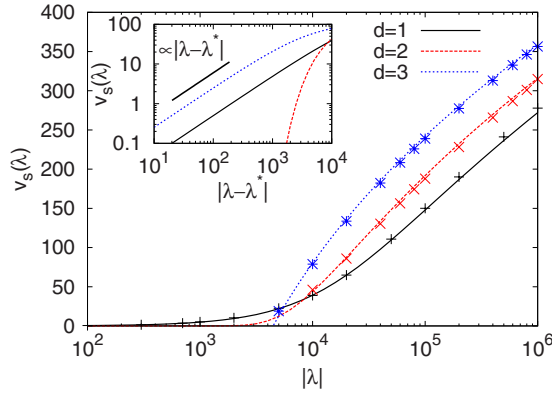
FIG. 4. (Color online) The steady-state velocity $v_s(\lambda)$ as a function of coupling constant $|\lambda|$ for one, two, and three spatial dimensions, determined theoretically (lines), compared to the square root of the slopes of the mean-square displacements at early times, $\partial\sqrt{\langle[\mathbf{r}_b(t)-\mathbf{r}_b(0)]^2\rangle}/\partial t$, for two and three dimensions (symbols) [cf. Figs. 2(b) and 2(c)]. Inset: the asymptotic solution of $v_s$ for small values of $|\lambda-\lambda^*|$, where we set $\lambda^*=0$ for $d=1,2$.

If noise is put on, again, the microbe is eventually disturbed in its steady-state motion. In one dimension, the microbe needs to overcome a barrier in order to change the direction of motion from left to right or vice versa, which renders the steady state very stable. As we were not able to observe long-time diffusive motion in one dimension for any coupling constant but always found ballistic motion within the time window accessible in computer simulations, we do not attempt to give a theoretical estimate of the diffusivity. In two or three dimensions, the picture is very different: the microorganism is only constrained in its motion parallel to its current trajectory, whereas it is free to move perpendicular to the same. During such transverse fluctuations the direction of the microbe's motion changes with the gradient of the chemical field.

In the following, we give a theoretical estimate of the microbe's long-time diffusivity in $d=2,3$ under the assumption of a fast relaxation of the chemical field, which is justified for $D_c\gg D$. In this case, the change in orientation is determined by the local, time-independent curvature $\kappa_0(\lambda)$ of the isodensity line (in two dimension) or surface (in three dimension) at the steady-state position $\mathbf{r}_s(t)$; the isodensity planes are defined by $\{\mathbf{r}^*(t)\,|\,\rho[\mathbf{r}^*(t),t]=\rho[\mathbf{r}_s(t),t]\}$. Locally, they have the form of a parabola (in two dimension) or of a paraboloid of revolution (in three dimension) and they move with the microorganism at the microorganism's velocity; this can be seen in Fig. 5, where a typical trajectory and the according chemical field at time $t$ is plotted for a microorganism in two dimensions.

Fluctuations transverse to the direction of motion lead to a mean transverse displacement $\langle\mathbf{r}_\perp^2(t)\rangle=2(d-1)Dt$, which, in turn, leads to a change in orientation of the velocity director $\mathbf{v}_b$ by a mean-square angle

$$\langle\theta^2(t)\rangle = \kappa_0^2\langle\mathbf{r}_\perp^2(t)\rangle = 2(d-1)D\kappa_0^2 t. \quad (18)$$

Exploiting that $\theta$ is Gaussian distributed, the average, normalized, and on the initial orientation $\mathbf{v}_b(t=0)$ projected velocity vector $\mathbf{v}_b(t)$ is given by
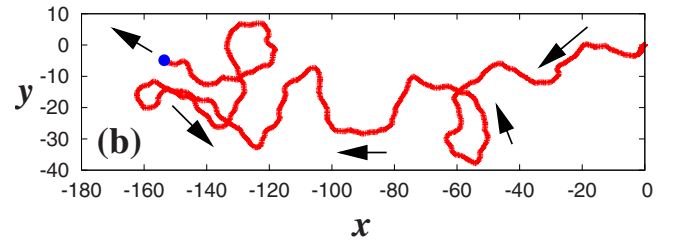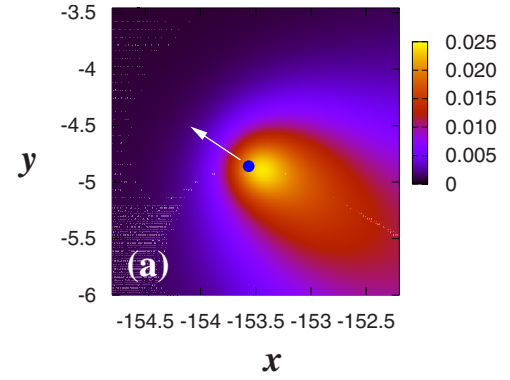




FIG. 5. (Color online) (a) Snapshot of the instantaneous density profile $\rho(x,y)$ of the chemorepellent released by the microorganism moving in two dimensions, obtained from simulation, at time instant $t=10.0$ (in units of $\lambda_e^{-1}$). (b) The entire trajectory, shown as the red (thick) curve, of the microorganism. The current position of the microorganism $\mathbf{r}_b(t)$ is indicated by the blue (black) dot in both the figures, and the direction of motion is indicated by arrows along the trajectory. The corresponding coupling strength being $|\lambda|=10000$.

$$\frac{\langle\mathbf{v}_b(t)\cdot\mathbf{v}_b(0)\rangle}{v_s^2} = \langle\cos[\theta(t)]\rangle = \exp\left[-\frac{\langle\theta^2(t)\rangle}{2}\right]. \quad (19)$$

Replacing time by arc length $s=v_s t$, the problem under study can therefore be mapped to the *wormlike chain* (WLC) model [4,16,36] of a polymer of a total arc length $L=v_s t$ and a persistence length, which is defined implicitly by $\langle\cos[\theta(t)]\rangle=\exp[-v_s t/l_p]$. Making use of Eqs. (18) and (19), the latter therefore reads $l_p=v_s/[(d-1)D\kappa_0^2]$. The mean-square end-to-end distance of the WLC for long chains $L\gg l_p$ is well-known [4,36] to be given by

$$\langle\mathbf{r}_b^2(t)\rangle \simeq 2Ll_p = \frac{2v_s^2 t}{(d-1)D\kappa_0^2}. \quad (20)$$

The long-time diffusivity of the microbe is then obtained as the time derivative of the mean-square end-to-end distance,

$$D_l(\lambda) = \frac{1}{2d}\frac{\partial\langle\mathbf{r}_\perp^2(t)\rangle}{\partial t} = \frac{v_s^2(\lambda)}{d(d-1)D\kappa_0^2(\lambda)}, \quad (21)$$

where we point out the $\lambda$ dependence of the steady-state velocity and the steady-state curvature. $D_l(\lambda)$ is plotted in Fig. 2(d) and compared to the results of the simulation.

It is ascertained from Fig. 2(d) that, in the limit of large $\lambda\gtrsim10^5$, the theory overestimates the diffusivity by a factor of $\sim3$, both in two and three dimensions, for the parameters $D=10$ and $t_0=0.001$, almost independent of $\lambda$. This discrepancy is attributed to the strong assumption of a constant,

nonfluctuating curvature $\kappa_0(\lambda)$ in Eqs. (18) and (21). Relaxing this assumption to fluctuating curvature with first and second moments $\langle\kappa\rangle=\kappa_0$ and $\langle(\kappa-\kappa_0)^2\rangle=\Delta\kappa^2$, which is further uncorrelated with the transverse displacement, i.e., $\langle\kappa(t)\mathbf{r}_\perp(t')\rangle=0$, the diffusion constant reduces to $D_l \rightarrow D_l/[1+(\Delta\kappa/\kappa_0)^2]$. Therefore, although we do not attempt to give an estimate of $\Delta\kappa$ here, the long-time diffusivity is expected to be smaller than in the "zeroth order" theory, Eq. (21), in agreement with the simulation results.

## V. CONCLUSION

In conclusion, we have explored the dynamics of autochemotaxis: a model microorganism is "smelling" its own secretion that is diffusing away. The microorganism follows the gradient [30] of its secreted chemical. For the attractive case, the mean-square displacement of the microorganism reveals a transient dynamical arrest, most pronounced in low spatial dimensionality. In the opposite case of chemorepulsion, there is a transient ballistic behavior, which crosses over to ultimate diffusion [37,38]. A simple theoretical analysis for large coupling strengths $\lambda$ reveals a scaling law for the long-time diffusion in the case of a chemoattractant, by regarding small excursions of the microbe's position about the bottom of an effective, time-dependent trapping potential. In the case of chemorepulsion, the microbe's trajectory was mapped to the contour of a wormlike chain, which gives a semiquantitative agreement with our computer simulations. The ranges of the coupling strength reported here are also easily obtainable in real experimental situations ($\lambda \sim 10^{-1}-10^4$), as estimated earlier in the text. We note that though the mechanism of temporal sensing [22,32,33] of chemoattractant or chemorepellent, which we do not consider here, is found in many small fast moving bacteria like *E. coli*; the direct gradient sensing mechanism is also present in microorganisms like the amoeba *Dictyostelium discoideum*, the yeast cell *Saccharomyces carevisiae*, lymphocytes, glial cells, and myxobacteria [28,30,31].

Chemotaxis in the gliding bacterium *M. xanthus* was demonstrated to be in response to self-generated signaling chemicals [39]. However, the diffusivity of the chemoattractant is significantly lower compared with the bacterial motility in this peculiar case. A numerical investigation [40] of a simple model case in one dimension compared the interplay between chemotaxis and chemokinesis mechanism with a concentration-dependent switching rate, showing crossover from suppressed to enhanced diffusion in the parameter space. This mean-field approach, studied in the limit of vanishing chemical diffusivity and chemical degradation rate, was based on the simplifying assumption that the chemical coupling only affects the frequency of direction reversal of the cell, keeping the cell speed unaltered.

Models of active colloids using surface reactions as a potential mechanism for self-propulsion have been proposed (see, e.g., Refs. [41,42]). In Ref. [41], the model *molecular machine* is a spherical colloid which reacts with the substrate at a specific site on its surface and self-propel by asymmetric release of the reaction product. The time evolution of the product particles is similar to that of chemical molecules emitted by a microorganism. Though the exact way of imparting a biased motion to the colloid by the emitted particles is very different from chemotactic coupling, such systems may also provide interesting situations to compare with our results. In fact, in Ref. [42], active colloids interacting with a self-generated cloud of solute were shown to have distinct propulsive and anomalous super-diffusive regimes preceding a final long-time effective diffusion. This is worth comparing with the ballistic to a modified diffusion crossover in our study on negative autochemotaxis.

Future work should focus on generalizing the model to a collection of model microorganisms [11], where hydrodynamic flow effects can play an important role [23,43,44] and steric repulsions can lead to aggregation and clumps [45] as known from active particles [24,46]. It would further be interesting to study the case of a geometric confinement of the particles [47–49] and the chemoattractant/repellent in order to see effects of a dimensional crossover. Finally, improving the theoretical approaches toward full quantitative agreement will be an important task for future research.

[1] M. Kollmann, L. Lovdok, K. Bartholome, J. Timmer, and V. Sourjik, Nature (London) **438**, 504 (2005).

[2] U. B. Kaupp, N. D. Kashikar, and I. Weyand, Annu. Rev. Physiol. **70**, 93 (2008).

[3] For a recent study, see, e.g., B. M. Friedrich and F. Jülicher, New J. Phys. **10**, 123025 (2008).

[4] M. Doi and S. F. Edwards, *The Theory of Polymer Dynamics*, 1st ed. (Clarendon Press, Oxford, 1986).

[5] J. K. G. Dhont, *An Introduction to Dynamics of Colloid* (Elsevier Science, Amsterdam, 1996).

[6] P. N. Pusey, in *Liquids, Freezing and the Glass Transition*, Proceedings of the Les Houches Summer School, edited by J. P. Hansen, D. Levesque, and J. Zinn-Justin, 1989 (North-Holland, Amsterdam, 1991), p. 763.

[7] W. C. K. Poon, *Soft Matter: From Synthetic to Biological Materials*, Lecture Notes of the 39th IFF Spring School (Forschungszentrum Julich GmbH, Germany, 2008), Vol. D11, pp. 1–15.

[8] M. T. Keating and J. T. Bonner, J. Bacteriol. **130**, 144 (1977).

[9] H. Hempel, M. Mieth, and L. Schimansky-Geier, *Nonlinear Physics of Complex Systems*, Lecture Notes in Physics (Springer, Berlin, 1996), Vol. 476.

[10] N. Mittal, E. O. Budreen, M. P. Brenner, and A. van Oudenaarden, Proc. Natl. Acad. Sci. U.S.A. **100**, 13259 (2003).

[11] F. Schweitzer and L. Schimansky-Geier, Physica A **206**, 359 (1994).

[12] Y. Tsori and P.-G. de Gennes, EPL **66**, 599 (2004).

[13] R. Grima, Phys. Rev. Lett. **95**, 128103 (2005).

[14] R. Grima, Phys. Rev. E **74**, 011125 (2006).

[15] As pointed out in Ref. [12], there is an analogy to polarons where self-trapping is thought of being a localization of electron due to the interactions with its own phonon cloud. Strictly speaking, such self-trapping transition does not exist as a thermodynamic singularity or as a true localization transition (see Refs. [50,51]), but it is only a property in the strong-coupling limit. This is similar to our dynamical findings here where perfect self-trapping only occurs at infinite coupling.

[16] B. M. Friedrich, Phys. Biol. **5**, 026007 (2008).

[17] L. Acedo, EPL **73**, 698 (2006).

[18] C. Sire and P.-H. Chavanis, Phys. Rev. E **78**, 061111 (2008).

[19] J. Sopik, C. Sire, and P.-H. Chavanis, Phys. Rev. E **72**, 026105 (2005).

[20] K. Zabrocki, S. Trimper, and M. Schulz, Int. J. Mod. Phys. B **22**, 1947 (2008).

[21] D. A. Clark and L. C. Grant, Proc. Natl. Acad. Sci. U.S.A. **102**, 9150 (2005).

[22] Y. Kafri and R. A. da Silveira, Phys. Rev. Lett. **100**, 238101 (2008).

[23] A. Shapere and F. Wilczek, Phys. Rev. Lett. **58**, 2051 (1987).

[24] J. Toner, Y. Tu, and S. Ramaswamy, Ann. Phys. (N.Y.) **318**, 170 (2005).

[25] L. Schimansky-Geier, M. Mieth, H. Rose, and H. Malchow, Phys. Lett. A **207**, 140 (1995).

[26] M. P. Allen and D. J. Tildesley, *Computer Simulation of Liquids* (Clarendon Press, Oxford, 1989).

[27] T. Hofer, J. A. Sherratt, and P. K. Maini, Physica D **85**, 425 (1995).

[28] M. Luca, A. Chavez-Ross, L. Edelstein-Keshet, and A. Mogilner, Bull. Math. Biol. **65**, 693 (2003).

[29] M. P. Brenner, L. S. Levitov, and E. O. Budrene, Biophys. J. **74**, 1677 (1998).

[30] R. G. Endres and N. S. Wingreen, Proc. Natl. Acad. Sci. U.S.A. **105**, 15749 (2008).

[31] P. J. M. van Haastert and M. Postma, Biophys. J. **93**, 1787 (2007).

[32] M. J. Schnitzer, Phys. Rev. E **48**, 2553 (1993).

[33] H. C. Berg and E. M. Purcell, Biophys. J. **20**, 193 (1977).

[34] T. J. Newman and R. Grima, Phys. Rev. E **70**, 051916 (2004).

[35] H. Risken, *The Fokker-Planck Equation, Methods of Solution and Applications*, 2nd ed. (Springer, Berlin, 1989).

[36] O. Kratky and G. Porod, Recl. Trav. Chim. Pays-Bas **68**, 1106 (1949).

[37] The Green's function for a case with nonzero chemical extinction rate ($\Lambda$) being known, it is not difficult to incorporate this into the equation of motion and simulate. The reason for considering $\Lambda=0$ is not only to study a case that is experimentally realizable (as in Ref. [8]), but also to examine the dynamics of the microbe when the effect of the chemical is most strongly felt. Even in this limit, we found a crossover to final diffusion. We therefore believe that the dynamics will not change qualitatively by setting a nonzero chemical extinction rate. Only the quantitative values of the crossover time scales, velocity, and long-time diffusivity are expected to shift because of the reduced effect of the chemical.

[38] For a similar behavior in two dimensions, see: X. L. Wu and A. Libchaber, Phys. Rev. Lett. **84**, 3017 (2000).

[39] D. B. Kearns and L. J. Shimkets, Proc. Natl. Acad. Sci. U.S.A. **95**, 11957 (1998).

[40] M. R. D'Orsogna, M. A. Suchard, and T. Chou, Phys. Rev. E **68**, 021925 (2003).

[41] R. Golestanian, T. B. Liverpool, and A. Ajdari, Phys. Rev. Lett. **94**, 220801 (2005).

[42] R. Golestanian, Phys. Rev. Lett. **102**, 188305 (2009).

[43] M. M. Hopkins and L. J. Fauci, J. Fluid Mech. **455**, 149 (2002).

[44] I. H. Riedel, K. Kruse, and J. Howard, Science **309**, 300 (2005).

[45] D. D. Holm and V. Putkaradze, Physica D **220**, 183 (2006).

[46] H. H. Wensink and H. Löwen, Phys. Rev. E **78**, 031409 (2008).

[47] S. van Teeffelen and H. Löwen, Phys. Rev. E **78**, 020101(R) (2008).

[48] S. E. Hulme, W. R. DiLuzio, S. S. Shevkoplyas, L. Turner, M. Mayer, H. C. Berg, and G. M. Whitesides, Lab Chip **8**, 1888 (2008).

[49] M. N. Popescu, S. Dietrich, and G. Oshanin, J. Chem. Phys. **130**, 194702 (2009).

[50] B. Gerlach and H. Löwen, Phys. Rev. B **35**, 4291 (1987).

[51] B. Gerlach and H. Löwen, Rev. Mod. Phys. **63**, 63 (1991).